Austrian Journal of Earth Sciences | Vienna | 2016 | Volume 109/1 | 99 - 113 | DOI: 10.17738/ajes.2016.0007

Hydrogeology and geothermic simulation of the geothermal doublet at Waldkraiburg (Bavaria)

Johann E. GOLDBRUNNER[1)] & Vilmos VASVÁRI[2)]

[1)] Geoteam Ges.m.b.H., Bahnhofgürtel 77/IV, 8020 Graz, Austria;

[2)] Ingenieurbüro für Kulturtechnik und Wasserwirtschaft, Kleegasse 4, 8020 Graz, Austria;

[*)] Corresponding author, goldbrunner@geoteam.at

KEYWORDS South German Molasse basin; Malm aquifer; geothermal use; geothermal doublet; numerical model

Abstract

For the geothermal project „Waldkraiburg" a well doublet was installed for district heating. The study area is located in the rural district of Mühldorf am Inn in Upper Bavaria, some 60 km east of Munich. Due to the intensive exploration activities of the petroleum and gas industry the geological structure of the subsurface is relatively well known.

Two deviated drillings, WKB Thermal 1 with a length of 2,839 m MD (2,720 m TVD), and WKB Thermal 2 with a length of 3,360 m MD (2,620 m TVD), were sunk into the fractured limestone-dolomite aquifer (Purbeck-Malm). The distance between the drillings at top aquifer amounts to 2,150 m. The evaluation of the hydraulic tests yields an aquifer transmissivity of 4 to $6x10^{-4}$ m²/s, and an aquifer thickness of 288 m. The fractured net thickness of the aquifer in WKB Thermal 1 amounts to 53 m (50 % in dolomite) and in WKB Thermal 2 to 44 m (77 % in limestone). The temperature of the minor mineralised water (c= 720 mg/l) at the well head is 106 °C. The temperature at the final depth of the wells corresponds to a geothermal gradient of 4.1 K/100 m. The basal heat flux at the top of the crystalline was estimated to be 0.097 W/m².

Based on the drilling data, on the geological profiles of the boreholes, and on the results of seismic investigations and structure maps, a 3D structural model was developed and implemented in a 3D flow and heat transport model.

After calibration and validation, the model was used to simulate the expected 50-year-operation and the subsequent hydraulic and thermal regeneration of the aquifer. The simulation verified that at a production/reinjection rate of 65 l/s and a reinjection temperature of 50 °C no thermal influence in the production well is to be expected during the operating period.

The range of the thermal influence (T > 1°C) in the middle of the aquifer around WKB Thermal 2 remains within a radius of 540 m. Temperatures at the reinjection site are expected to return to levels greater than 100 °C after a period of 2,300 years.

Im Rahmen des Geothermieprojektes „Waldkraiburg" errichteten die Stadtwerke Waldkraiburg GmbH eine Dublette zur Nutzung von geothermalen Wässern aus dem tieferen Untergrund für die Nah- und Fernwärmeversorgung. Das Untersuchungsgebiet des Projektes liegt im Landkreis Mühldorf am Inn, in Oberbayern ca. 60 km östlich von München. Durch die intensive Erdöl- und Erdgasexplorations- und -fördertätigkeit war der geologische Aufbau des Gebietes relativ genau bekannt.

Die zwei abgelenkten Bohrungen, WKB Thermal 1 mit einer Länge von 2839 m MD (2720 m TVD) und WKB Thermal 2 mit einer Länge von 3360 m MD (2620 m TVD) wurden in den geklüfteten Kalkstein-Dolomit-Aquifer (Purbeck-Malm) abgeteuft. Die Entfernung der Bohrungen bei Top Aquifer beträgt 2150 m. Die Auswertung der hydraulische Tests ergab eine Transmissivität des Aquifers von T = 4 bis $6x10^{-4}$ m²/s bei einer Mächtigkeit von 288 m. Die geklüftete Gesamt-Nettomächtigkeit des Aquifers in WKB Thermal 1 beträgt 53 m (50 % im Dolomit) und in WKB Thermal 2 44 m (77 % im Kalkstein). Die Temperatur des gering mineralisierten Wassers (c= 720 mg/l) am Brunnenkopf beträgt106 °C. In den Bohrungen wurde ein geothermischer Gradient von 4,1 K/100 m ermittelt. Der basale Wärmefluss am Top Kristallin konnte mit 0.097 W/m² abgeschätzt werden.

Auf Basis von Bohrdaten, der Bohrergebnisse der abgeteuften Bohrungen, der Ergebnisse der seismischen Untersuchungen und der Strukturkarten wurde ein 3D-Strukturmodell des Gebietes erstellt und in einem 3D-Strömungs- und Wärmetransportmodell implementiert.

Mit Hilfe des kalibrierten und validierten Modells wurden der 50jährige Betrieb und die anschließende hydraulische und thermische Regeneration des Aquifers simuliert. Die Simulationsergebnisse zeigen bei einer Förderung von 65 l/s und einer Reinjektionstemperatur von 50°C keine thermische Beeinflussung der Förderbohrung während der Betriebsdauer. Der Wirkungsbereich der thermischen Beeinflussung (ΔT > 1°C) in Aquifermitte liegt um WKB Thermal 2 in einem Umkreis von r = 540 m. Eine Wiedererwärmung des Wassers über 100 °C ist nach ca. 2300 Jahren zu erwarten.

1. Introduction

The South German Molasse Basin is one of the most prospective areas for the generation of hydro-geothermal energy in Germany. According to the data presented by Agemar et al. (2014) 15 geothermal district heating projects with an installed thermal capacity of 190.5 MW have been implemented to date. Waldkraiburg (population 22,500 in late 2013), situated

some 60 km east of Munich, is the largest city in the Upper Bavarian county of Mühldorf. Based on an existing district heating system, a geothermal utilization system was begun in 2012. The district heating network was expanded gradually and reached a thermal power of 4.2 MW by the end of 2014, based on a flow rate of max. 28 l/s. The maximum recorded temperature at the wellhead in well WKB Th1 was 106 °C. The final capacity of the installation is expected to amount to 14 MW and will require a flow rate of some 60 l/s.

The assessment of the sustainability of a geothermal doublet is of great importance for the prediction of the lifetime of a geothermal plant. Hydraulic and thermal simulations are a well-recognized procedure for assessing the economic viability of such plants and are accepted by the mining authorities as a tool for dimensioning the licence area for exploitation.

The present paper describes the technical design and the developed stratigraphy of the two drillings in Waldkraiburg, and also describes the hydraulic properties of the Malm aquifer. A 3D structural and a conceptual model are developed based on previous drilling and seismic data, on structural maps, and on current drilling results. After translating the conceptual model into a numerical model, the calibration and validation process are then outlined. Finally, the simulation of the doublet operation is carried out for the 50 year operating period, and the results, complete with sensitivity analysis, are then discussed.

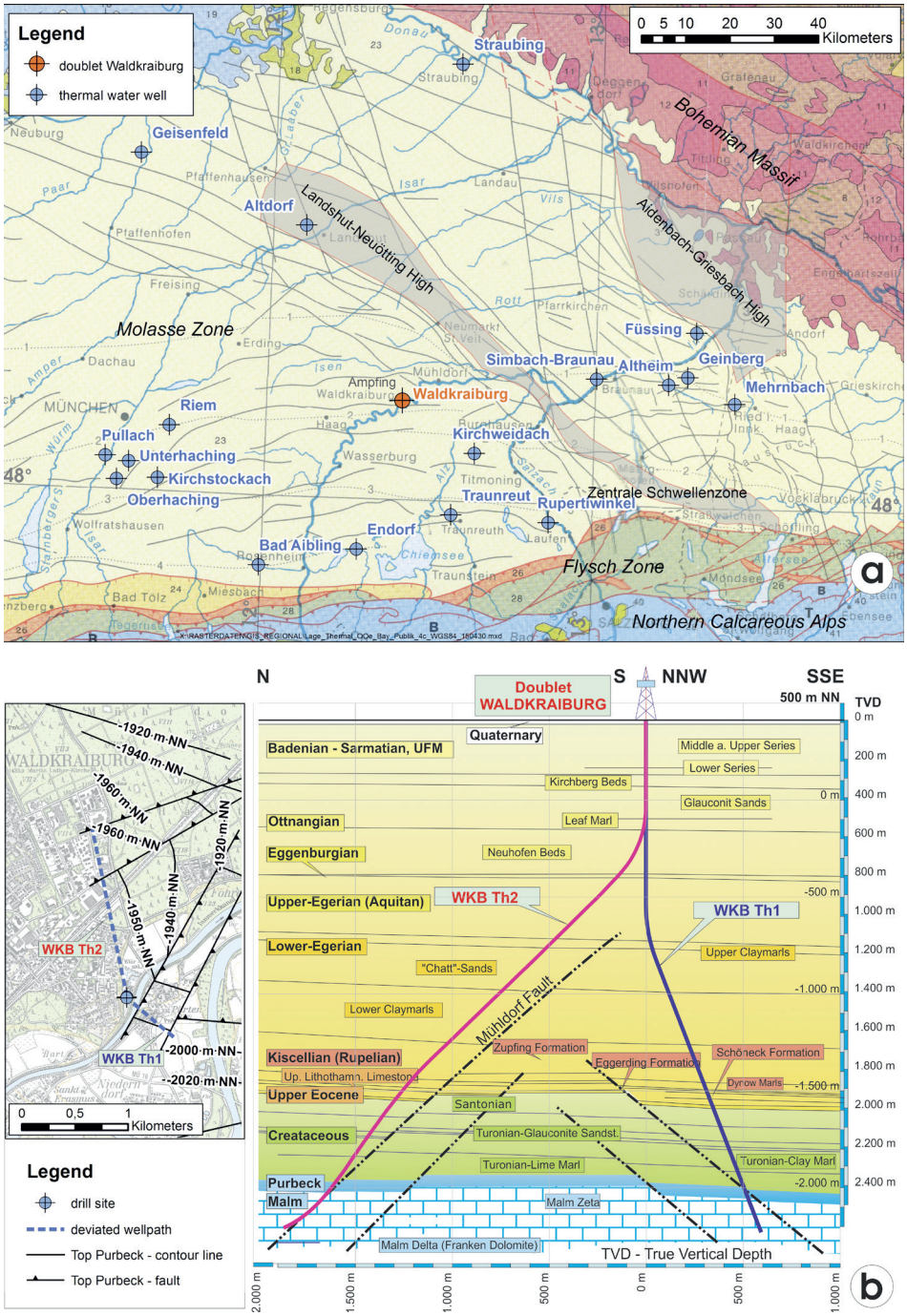

Figure 1: Location of wells, geological background (after GBA, 2013) (a) and geological profile of the doublet WKB Th1 and WKB Th2 (b).

2. Geological setting

The South German Molasse Basin is part of the foreland basin stretching from Switzerland in the West to Lower Austria in the East. The basin has an asymmetric cross section with the deepest parts lying along the Alpine thrust front in the SE. Waldkraiburg is situated in the eastern part of the Wasserburg Depression and lies at a distance of some 40 km from the northern tectonic rim of the Alps (Figure 1). The Molasse Basin comprises Late Eocene to Late Miocene sediments of a maximum thickness of 5,000 m. At Waldkraiburg the thickness is some 2,000 m. In general, the permeable sequences within the Molasse sediments, such as the Chattian Sands, are not suitable for geothermal use on a large scale (i.e. > 1 MW). The main aquifer for geothermal exploration and exploitation is located in the Upper Jurassic carbonate rocks of the pre-tertiary basin floor. The Malm formation is generally explored as a fractured and faulted reservoir since facies-based approaches have proved unsuccessful. In the Eastern part of the Wasserburg

	WKB Th1	WKB Th2
End depth [m MD]	2,840	3,360
End depth [m TVD]	2,718	2,620
Depth difference MD – TVD [m]	122	740
Max. inclination [°]	30	65
Azimuth [°]	132	350
Horizontal distance at final depth [m]	639	1,865

Table 1: Main technical data of the deviated drillings WKB Th1 and WKB Th2.

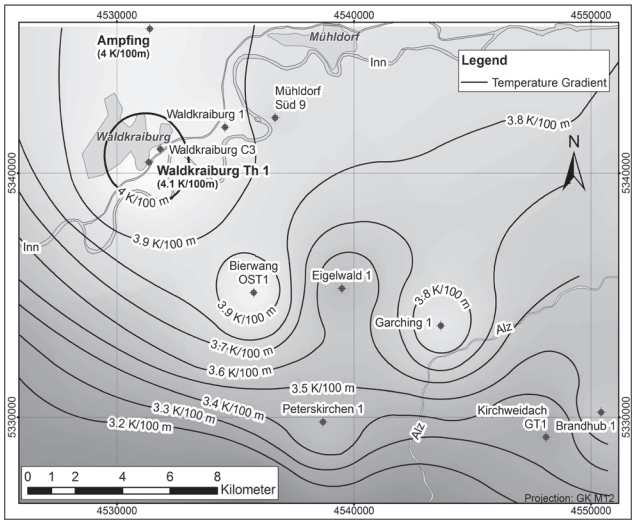

Figure 2: Geothermal gradients in the Waldkraiburg area.

Depression the Malm carbonate rocks reach a thickness of some 500 m. The hydraulic conductivity distribution (as T/H in m/s) of the Malm aquifer in the South German Molasse Basin is mapped by Birner et al. (2012) and indicates a hydraulic conductivity in the order of 10-6 m/s in the Inn region at Waldkraiburg. Only a few drillings have penetrated the entire thickness of the Malm in this part of the Molasse basin. This is due to the fact that in the south of the basin the basin floor lies at depths of more than 5,000 m.

Due to the proximity to the hydrocarbon fields of Ampfing, Mühldorf-Süd and Waldkraiburg, data on the geological and structural setting of the Neogene and Paleogene strata were readily available for the study area (Unger, 1978). Most of the hydrocarbon exploration boreholes targeted the Chattian Sands and Upper Eocene sandstones and limestones respectively, but only the hydrocarbon well Ampfing 1 hit the geothermal target horizon. Top of Purbeck was reached at 2,304 m in this well. The borehole penetrated Purbeck and Malm down to the Frankendolomit and had to be abandoned at 2,776 m due to technical problems.

Two reflexion seismic profiles from the hydrocarbon exploration were used in designing the geothermal drilling project and in defining targets. Evaluation of these profiles revealed the presence of a favourable structure formed by synthetic and antithetic faults in the Mesozoic subsurface to the South of Waldkraiburg. The antithetic fault in the north is part of a regional structure which can be traced from Anzing in the West to Mühldorf in the east (Kraus, 1968). This fault, with a maximum throw of 150 m, is named the „Mühldorf fault" and is an important structure in the trapping of oil in the Eocene limestones and sandstones, and in the trapping of gas in the Chattian Sands.

The identified faults formed the major targets for the deviated geothermal drillings which were carried out between August 2010 and March 2011. The main technical data are presented in Table 1. A geothermal gradient of 4 K/100 m was expected based on reliable temperature measurements of the oil produced in the Ampfing oil field (Mietens, 1966), thus allowing production temperatures of over 100 °C. Figure 2 presents a map of geothermal gradients in the Waldkraiburg area and its surroundings, indicating a local anomaly based on the temperature data of the Waldkraiburg geothermal wells.

The casing design was laid out for a flow rate of some 80 l/s. This requires a diameter of 6" in the aquifer. After testing, WKB Th1 was designated as the production well, and WKB Th2 as the reinjection well of the doublet.

The lithostratigraphic classification of the drilled sections was based on cuttings analyses and geophysical logging, and on correlation with the stratigraphy of the hydrocarbon wells (Table 2).

Waldkraiburg Th1 (WKB Th1) has drilled 275 m of Malm (Delta to Zeta), which corresponds to a vertical thickness of 257 m. Top Malm was tapped at 2,461 m TVD. The cumulative length of the dolomitic sections within the carbonate section amounted to 80.2 m. The dolomites were white to off-white, fine to micro-crystalline; sugar grained sections were observed. Permeable sections were discretized based on evaluation of the Sonic, Density and the Dual Laterolog and the rate of penetration (d-exponent), resulting in a cumulative length of 53 m of the pay zone. The individual thickness of the permeable horizons ranges from 0.4 to 11.7 m. Some 50 % of the permeable horizons are in dolomite.

Waldkraiburg Th2 (WKB Th2), which was deviated towards the North, tapped Top Malm at a TVD of 2,430 m and drilled 304 m of Malm which corresponds to a vertical thickness of 189 m. Permeable sections were deduced from Dual Laterolog, Caliper log and the rate of penetration (d-exponent). Of 44 m total length of permeable horizons only 23 % were in dolomites.

The temperatures were determined to be as high as 119 °C and 120 °C respectively at the end depth of the two boreholes. During air lift tests a maximum temperature of 112 °C was recorded at 3,000 m MD (2,385 m TVD; 45 m above Top Malm) in Well WKB Th1. During current operation, temperatures up to 110 °C have been measured at the centrifugal pump at a depth of 150 m. These values correspond to a geothermal gradient of 4.1 K/100 m at Waldkraiburg.

The deep groundwater at Waldkraiburg is of the sodium-(calcium)-bicarbonate-chloride type with a TDS of about 0.7 g/l. Data from water analyses executed in WKB Th1 are summarized in Table 3.

This level of mineralization is typical of the Malm deep ground waters found in the Munich area (Stober et al., 2014)

Stratigraphic unit	WKB Th2		WKB Th1		Difference	
	to	thickness	to	thickness	depth	thickness
	m TVD	m	m TVD	m	m	m
Quaternary - Pürten Terrace	**18.0**	**18.0**	**18.0**	18.0	-	-
Badenian - Sarmatian,						
Upper Freshwater Molasse	**277.5**	**259.5**	**277.5**	259.5	-	-
Middle and Upper Series	246.0	228.0	244.5	226.5	- 1.5	- 1.5
Lower Series	277.5	31.5	277.5	33.0	-	1.5
Ottnangian	**791.0**	**513.5**	**792.0**	514.5	1.0	1.0
Kirchberg Beds	340.0	62.5	340.0	62.5	-	-
Glauconitic Sands	514.0	174.0	507.0	167.0	- 7.0	- 7.0
Leaf marl	568.0	54.0	564.0	57.0	- 4.0	3.0
Neuhofen beds	791.0	223.0	792.0	228.0	1.0	5.0
Eggenburgian	**808.0**	**17.0**	**812.0**	20.0	4.0	3.0
Upper Egerian (Aquitan)	**1,1320**	**324.0**	**1,135.0**	323.0	3.0	- 1.0
Lower-Egerian	**1,654.0**	**522.0**	**1,672.0**	537.0	18.0	15.0
Upper Claymarls	1,174.0	42.0	1,179.0	44.0	5.0	2.0
Chatian Sands	1,395.0	221.0	1,402.0	223.0	7.0	2.0
Lower Claymarls	1,654.0	259.0	1,672.0	270.0	18.0	11.0
Kiscellian (Rupelian)	**1,889.5**	**235.5**	**1,922.0**	250.0	32.5	14.5
Zupfing Formation	1,832.0	178.0	1,868.0	196.0	36.0	18.0
Eggerding Formation	1,870.5	38.5	1,904.0	36.0	33.5	- 2.5
Dynow Marls	1,877.0	6.5	1,910.0	6.0	33.0	- 0.5
Schöneck Formation	1,889.5	12.5	1,922.0	12.0	32.5	- 0.5
Upper Eocene	**1,966.0**	**76.5**	**1988.0**	66.0	22.0	- 10.5
Upper Lithothamnian limestone	1,941.0	51.5	1,956.0	34.0	15.0	- 17.5
Ampfing Beds/glauconitic limestone	1,966.0	25.0	1,988.0	32.0	22.0	7.0
Cretaceous (Upper and Lower Cretaceous)	**2,381.0**	**415.0**	**2.413.5**	425.5	32.5	10.5
Santonian	2,016.0	50.0	2,075.5	87.5	59.5	37.5
Coniacian – clay marl	2,116.0	100.0	2,170.0	94.5	54.0	- 5.5
Coniacian – lime marl	2,143.0	27.0	2,200.0	30.0	57.0	3.0
Turonian – glauconitic sandstone	2,154.0	11.0	2,214.5	14.5	60.5	3.5
Turonian – clay marl	2,256.0	102.0	2,308.0	93.5	52.0	- 8.5
Turonian – lime marl	2,342.0	86.0	2,389.0	81.0	47.0	- 5.0
Gault sands	2,357.5	15.5	2,407.0	18.0	49.5	2.5
deeper parts of lower Cretaceouse	2,381.0	23.5	2,413.5	6.5	32.5	- 17.0
Purbeck	2,430.0	49.0	2,461.0	47.5	31.0	- 1.5
Malm	2,619.0	189.0	2,718.0	257.0	99.0	68.0
Malm Zeta	2,619.0	189.0	2,684.0	223.0	65.0	34.0
Malm Delta (Franconian Dolomite)			2,718.0	34.0		

Table 2: Stratigraphic structure of the drillings WKB Th1 and WKB Th2.

and is distinctly lower than that of the Malm waters in the Lower Bavarian – Upper Austrian part of the Molasse Basin east of the Landshut-Neuötting High and the Central Swell, where sodium-bicarbonate-chloride waters with a TDS of 1 to 1.2 g/l are common (Goldbrunner, 2012).

3. Conceptual model

Since natural hydrogeological boundaries could not be defined within the model area, the boundaries of the model in the north and south were defined by means of fault lines (the Ampfing fault and Bierwang fault respectively). To the east, the structure bordering the Landshut-Neuötting High forms an important boundary as the Malm Aquifer is bounded on the east by the uprising basement crystalline rocks. The W model boundary was defined arbitrarily by an N-S trending line.

Nine litho-stratigraphic units were considered in the model. The upper and lower limiting surface are the surface area

			Date of sampling	
Parameter		**Unit**	**04.10.2011**	**18.12.2012**
temperature		[°C]	98.4	17.6
pH		[-]	6.5	7.14
EC	(25 °C)	[µS/cm]	741	719
Cations				
Ammonium	NH_4^+	[mg/l]	1.3	0.69
Sodium	Na^+	[mg/l]	115	112.40
Potassium	K^+	[mg/l]	18	15.40
Calcium	Ca^{2+}	[mg/l]	27.1	40.10
Magnesium	Mg^{2+}	[mg/l]	5.4	5.20
Strontium	Sr^{2+}	[mg/l]	0.8	0.93
Manganese	Mn^{2+}	[mg/l]	0.06	0.10
Iron II and III	Fe^{3+2+}	[mg/l]	0.13	2.62
Sum cations		**[mg/l]**	**167.79**	**177.44**
Anions				
Fluoride	F^-	[mg/l]	2.9	1.957
Chloride	Cl^-	[mg/l]	81.4	86.7
Bromide	Br-	[mg/l]	0.4	0.25
Sulphate	SO_4^{2-}	[mg/l]	4.8	2.015
Hydrogen carbonate	HCO_3^-	[mg/l]	288	311.5
Sulphide tot.	HS^-. S^{2-}	[mg/l]	2.2	
Hydrogen sulphide	HS-	[mg/l]		6.17
Sum anions		**[mg/l]**	**379.7**	**408.88**
Undissociated substances				
m-silicic acid	H_2SiO_3	[mg/l]	130	133.9
Total dissolved solid TDS		**[mg/l]**	**677.49**	**720.22**

Table 3: Hydrochemical results of well WKB Th1.

and a level at -4,000 m b.m.s.l (= m NN in Germany) in the crystalline basement.

The lack of a sufficient number of hydraulic parameters for the different layers in the model area meant that data from existing validated models of the Bavarian and Upper Austrian Molasse Basin (Goldbrunner et al., 2008; Wenderoth and Huber, 2011; Dussel et al., 2012) had to be used. The hydraulic parameters are presented in Table 4.

The Malm sequence was divided into two layers. In the upper part, including Purbeck, higher permeabilities were assigned compared to the deeper part. In accordance with other models (Wenderoth and Huber, 2011; Dussel et al., 2012) fault zones in Malm are generally shown as zones of increased hydraulic conductivity.

The fault zones were simplified for purposes of numerical modelling by only considering faults with significant throws. For the numerical simulation,

Hydro-stratigraphic unit	**Lithology**	**Hydraulic classification of strata**	**Thickness [m]**	**Hydraulic conductivity [m/s]**	**Specific Storage [-]**
Upper Freshwater Molasse (incl. Quaternary)	gravel, carbonate sandstones	aquifer/ aquiclude	278	$1x10^{-5}$	$1x10^{-9}$
Neogene	sand, marl, sandstone	aquiclude	535	$1x10^{-8}$	$1x10^{-9}$
Lower-Egerian, Kiscellian	argillaceous marl, sand, marlstone, claystone	aquiclude	1,110	$1x10^{-8}$	$1x10^{-9}$
Eocene	Lithothamnium limestone, glauconitic marlstone	aquiclude	66	$1x10^{-8}$	$1x10^{-9}$
Cretaceous	argillaceous marl, carbonate marl	aquiclude	426	$1x10^{-8}$	$5x10^{-7}$
Purbeck/Upper Malm Undisturbed	limestone/dolomite	aquifer	305	$1\text{-}2x10^{-6}$	$3x10^{-7}$
Purbeck/Upper Malm fault zone	limestone/dolomite	aquifer	305	$3x10^{-6}$	$3x10^{-7}$
Lower Malm undisturbed	Limestone	aquifer	140	$1x10^{-7}$	$4x10^{-7}$
Lower Malm fault zone	limestone/dolomite	aquifer	140	$1x10^{-7}$	$4x10^{-7}$
Crystalline Basement undisturbed	orthogneiss	aquiclude	>100 m	$1x10^{-8}$	$1x10^{-9}$

Table 4: Hydraulic properties of the hydro-stratigraphic units (after Stober 1995; Goldbrunner et al. 2008; Wenderoth and Huber, 2011; Dussel et al., 2012).

the Mühldorf fault with its well-documented inclination was employed, together with the other fault zones, which were displayed vertically. Vertical fault offsets distinctly less than the thickness of the affected block, have a negligible effect on the flow in the block so this simplification of model geometry is acceptable with regard to the hydraulic behaviour of the aquifer.

Structural maps were generated for the formation tops of the Chattian sands, Cretaceous, Purbeck/Malm, and Malm Gamma („Lower Malm"). They were converted to a geological 3D-model using the „fault-block" method (Jones et al., 1986). The total area was divided into so-called fault blocks. The individual blocks, which are predominantly confined by faults, were depicted by polygonal lines. The residual edges were treated as faults without offsets. The polygonal chains and the data points (depths) were digitalised. Subsequently, the individual blocks per layer surface were separately subjected to a gridding process. For each block, a grid and related isolines were created. Finally, the contours of the individual blocks were plotted in a collective map. The three-dimensional acquisition, processing and visualization of geological structural data was performed using the ArcView v. 10.1 program from ESRI, in particular with the module 3D Analyst.

4. Numerical model

The main purpose of the hydraulic and thermal simulations model was to quantify the possible mutual thermal and hydraulic influence of WKB Th1 and WKB Th 2 over the prospective operating period of 50 years and to describe the regional impact of heat mining.

The numerical flow and heat transport model was developed with the help of the software FEFLOW version 6.1 (DHI-WASY, 2010; Diersch, 2014). The simulation with FEFLOW is based on the coupled solving of the differential equation of the groundwater flow and the heat transport. The governing equations for the common case of the three-dimensional flow and heat transport can be written as follows (De Marsily, 1986; Bundschuh and Suárez Arriga, 2010; Diersch, 2014]:

Groundwater flow

$$\nabla\left[p \cdot \frac{\mu_0}{\mu} K\left(\nabla h_0 \frac{p_w - p_{w,0}}{p_{w,0}} \nabla z\right)\right] = p_w \cdot S_{s,0} \frac{\partial h_0}{\partial t} - p_s \cdot q_s \qquad (1)$$

Heat transport

$$\left(1+\frac{1-n}{n}\cdot\frac{p_R}{p_w}\cdot\frac{c_R}{c_w}\right)\frac{\partial(nT)}{\partial t} = \nabla\left[n\left(\frac{1-n}{n\cdot p_w\cdot c_w}+\alpha\frac{q}{n}\right)\cdot\nabla T\right] - \nabla\cdot(q\cdot T) - qwT \qquad (2)$$

where

∇ = nabla-operator $\left(\frac{\partial}{\partial x}, \frac{\partial}{\partial y}, \frac{\partial}{\partial z}\right)$

x, y, z = Cartesian coordinates [m]
μ = dynamic viscosity of water [N·s/m²]
μ_0 = dynamic viscosity of water at reference temperature and concentration [N·s/m²]
k_0 = hydraulic conductivity of aquifer for model water [m/s]
h_0 = hydraulic head referred to model water [m]
p_R = density of rock [kg/m³]
p_w = density of water [kg/m³]
$p_{w,0}$ = density of model water [kg/m³]
$S_{s,0}$ = specific storage coefficient [kg/m³]
q_s = sink or source of water [1/s] with density of p_w
c_R = specific heat capacity of rock [J/(kg•K)]
c_w = specific heat capacity of water [J/(kg•K)]
T = temperature [K]
T_s = temperature of source [K]
t = time [s]
n = porosity [-]
α = dispersivity [m]
λ = thermal conductivity of aquifer (rock + water)[W/m•K]
q = specific flow rate [m/s]

4.1 Model geometry and mesh

The model area corresponds to that of the 3D conceptual model and was discretised in two steps. First, a horizontal discretisation was carried out by means of triangular elements. This model mesh with element sizes between 0.15 m and 500 m captures the morphologically important and hydraulically effective structures (faults) as well as the well locations of the doublet according to the conceptual model (Figure 3).

The deviated boreholes WKB Th1 and WKB Th2 were realised in the model as vertical wells with a location corresponding to the barycentre of the borehole path deviated in the Malm. The permissibility of the vertical approximation of deviated drillings in regional models in respect to the hydraulic and thermal interaction of neighbouring wells was demonstrated by Dussel et al. (2012).

The 9 layers of the 3D geologic structural model were split into top Malm (Purbeck), top Malm Gamma and top Crystalline in order to facilitate the retracing of the vertical flow and transport processes. Thus, in the numerical model, 28 layers are present (Table 5). The number of the triangular elements per model layer amounts to 207,316 resulting in a total of 5,804,848 prismatic elements (Figure 3).

4.2 Hydraulic parameters

Prior to numerical modelling the hydrogeological and hydrostratigraphic units were delineated. Units with similar hydraulic properties were merged. The differentiated units and their hydraulic parameters are shown in Table 4.

In a first approach, hydraulic parameters for the different stratigraphic units were taken from validated hydraulic-thermal models from the Lower Bavarian/Upper Austrian border region (Goldbrunner et al. 2008; Wenderoth and Huber, 2011; Dussel et al., 2012). The Malm was divided into two layer packages where the top section, which also comprises the Purbeck layers, was assigned higher hydraulic conductivities than the underlying sections. In accordance with other models, the faults in the Malm were more highly weighted hydraulically, and in general, they were designated as zones of enhanced hydraulic conductivity (2 to 3 times higher than

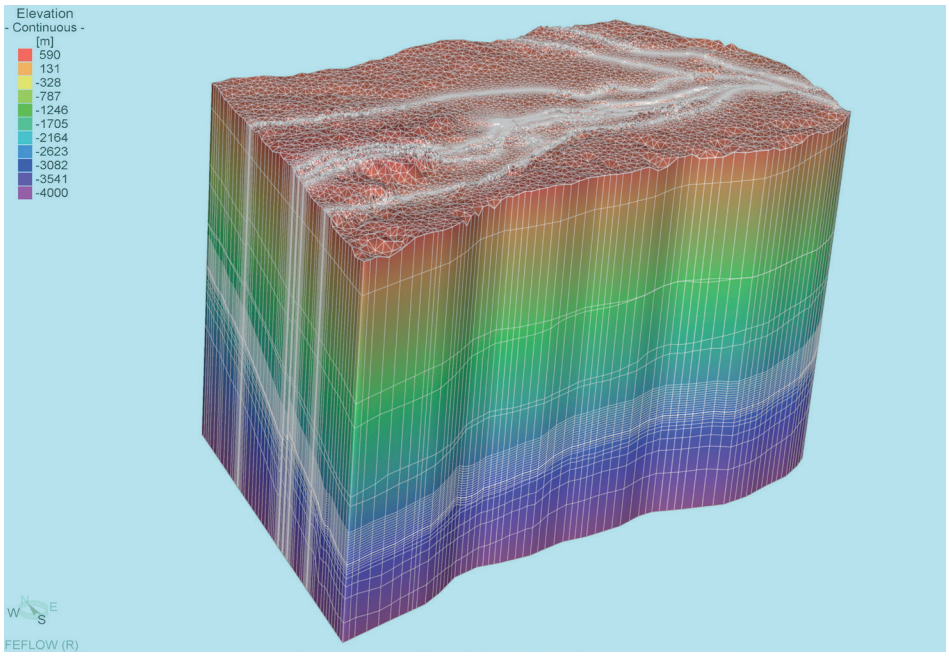

Figure 3: 3D structural model and model mesh with 28 model layers (V.E. 5x).

Model layer boundary		Model slice	Depth (m NN)	Stratigraphy	Model layer
1	Top ground surface	1	370 to 590	Quaternary	1
2	Base, roof sediments of Chattian Sands	2	109 to 254	Upper Freshwater Molasse	2
3	Top Chattian	3	-1,115 to - 501	Neogene	3
4	Base Chattian	4	-1,397 to -553	Lower-Egerian, Kiscellian	4
5	Top Eocene	5	-2,218 to -1,040	Eocene	5
6	Top Cretaceous	6	-2,338 to -1,090	Cretaceous	6 to 9
		7 to 9			
7	Top (shallow) Malm	10	-2,752 to -1,090	Purbeck and Upper Malm	10 to 23
		11 to 22			
8	Top (deep) Malm	23	-3,153 to -1,246	Lower Malm	24 to 25
		24 to25			
9	Top Crystalline	26	-3,357 to -1,392	Crystalline	26 to 28
		27 to28			
10	Base Crystalline	29	-4,000		

Table 5: Numerical model – vertical model resolution (28 model layers).

that of undisturbed areas). For the Mühldorf fault, intersected by well WKB Th2, this approach could not be applied as the productivity/reinjectivity of this well is lower than in WKB Th1.

Table 6 summarizes the transmissivities determined by hydraulic test evaluation.

Evaluation of the different pumping tests or test phases yielded a regional transmissivity of T = 4 to 6x10^{-4} m^2/s for the Malm aquifer. By taking a total aquifer thickness, tested in the open holes, of 288 m, a horizontal hydraulic conductivity of k = 1.4 to 2.1x10^{-6} m/s was used for the hydraulic calibration of the model. In the Malm aquifer an anisotropy factor of 5 (k_{xx} = k_{yy} = 5·kzz) between the vertical and lateral hydraulic conductivity was assumed. No anisotropy was considered in the adjacent layers.

4.3 Hydraulic head conditions

Because of the small number of wells in the eastern part of the Molasse Basin the regional distribution of the hydraulic head in the Malm aquifer is not perfectly clear. The first trans-regional aquifer potential plan was created by Lemcke (1988) and was based primarily on information from hydrocarbon exploration wells. This hydraulic head plan is now considered outdated. A potential plan for the Malm aquifer based on uniform conditions (T = 10 °C and c = 500 mg/l) was published by Frisch and Huber (2000). Based on this plan, and on regional considerations, a potential of 390 m NN can be assumed for Waldkraiburg. The general flow direction in the Waldkraiburg area is SE-NW directed, but local flow directions cannot be deduced. Furthermore, in the hydrogeological map of Bavaria (Wagner et al., 2009) potential lines for the Waldkraiburg area are not represented either.

A flat potential surface was thus assumed for the model area as an initial condition. The potential was derived from the initial head measurements in the wells WKB Th1 and WKB Th2. The potentials for the model water and for the thermal water are presented in Table 7. The potential at WKB Th1 is regarded as more reliable and was thus taken for the simulation due to the fact that the pressure gauge here was situated closer to the top aquifer than in WKB Th2. (For the calculation of potentials in Table 7 the following values were used: model water: T = 10 °C, p = 1 bar, c = 500 mg/l; pw = 1000.227 kg/m³; thermal water: T = 106 °C, pm = 113 bar, c = 720 mg/l; pw = 959.220 +0.720 = 959.94 kg/m³.)

The assumption of a flat potential surface in the model area implies that the advective transport of the thermally influenced water may be neglected. This means that with

Evaluation method	Transmissivity [m²/s]				
	short-time pumping test		pumping- and reinjection test		
	WKB Th1	WKB Th2	WKB Th1 phase 3	WKB Th1 phase 4 and 5	WKB Th2
THIEM drawdown / pressure rising	$4.55x10^{-4}$	$2.66x10^{-4}$	-	-	$2.72x10^{-4}$
THEIS drawdown	-	-	$4.4x10^{-4}$	$4.8x\ 10^{-4}$	-
COOPER & JACOB drawdown	-	-	$4.1x10^{-4}$	$4.9x10^{-4}$	-
THEIS & JACOB recovery	$4.35x10^{-4}$	$5.9x10^{-4}$	$5.4x10^{-4}$	$6.0x10^{-4}$	-

Table 6: Results of the hydraulic tests evaluated.

Well	Initial pressure [bar]	Measuring depth [m TVD]	Measuring depth above Top Purbeck [m]	Potential model water [m NN]	Potential thermal water [m NN]
WKB Th1	225.53	2,363	50.5	347.06	443.52
WKB Th2	185.10	1,937	444	361.02	440.19

Table 7: Initial pressures and potentials in the wells WKB Th1 and WKB Th2.

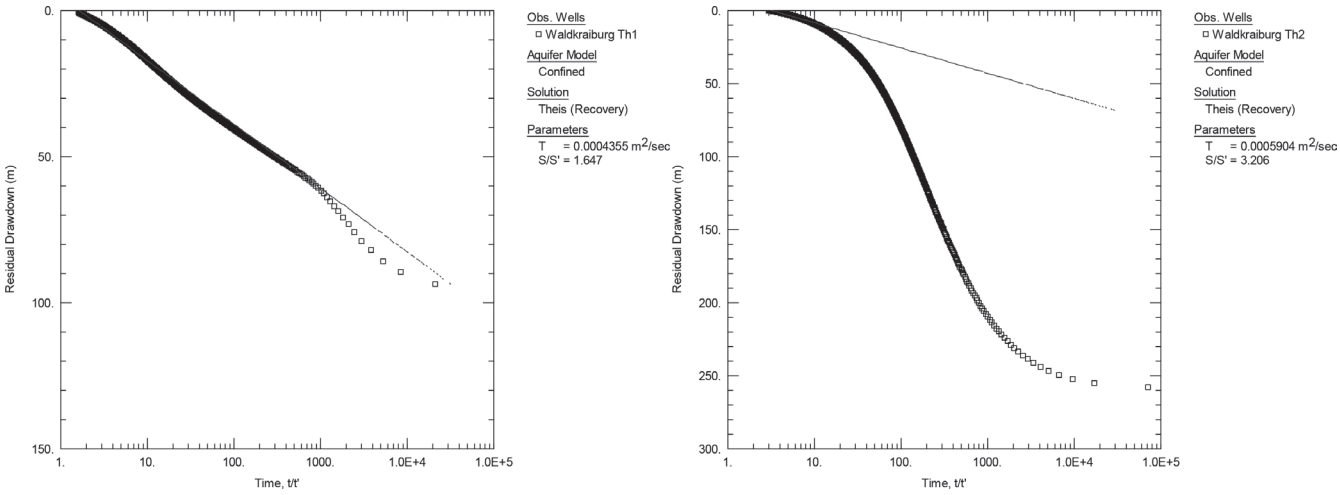

Figure 4: Evaluation of the recovery in WKB Th1 (left) and WKB Th2 (right) after the short-time pumping tests.

respect to cold plume propagation, underestimation occurs in the flow direction of the groundwater, while overestimation occurs against it.

However, as in the vicinity of the doublet, the groundwater flow is dominated by the high potential gradients generated by the extraction and reinjection operation, the neglect of the natural groundwater flow is an acceptable approach. Only after ending the doublet's operation, i.e. during the thermal regeneration of the aquifer, would the natural groundwater flow have an effect on the cold water plume.

4.4 Calibration and validation of the flow model

For the hydraulic calibration of the model the following pumping tests and other hydraulic tests were used:

- Short-time pumping test in WKB Th1 – monitoring WKB Th2 (12.-14.07.2011)
- Short-time pumping test in WKB Th2 – monitoring WKB Th1 (20.-23.07.2011)
- Pumping and reinjection test in WKB Th1 and Th2, 3rd phase (05.-08.09.2011)
- Test operation, pumping in WKB Th1 and reinjection in WKB Th2 (10.10.2012-31.01.2014)

The evaluation of the recovery periods after both short-time pumping tests is shown in Figure 4.

The calibration was made using a flow model with no coupling between the density and viscosity dependent heat transport model. At first the Q – dp diagrams were plotted in order to check the measured pressure drawdown and pressure rise values for consistence and plausibility (Figure 5 and 6). This process led to the following conclusions and procedure.

At well WKB Th1 calibration was based on the results derived from the first step of the pumping test. The validation was carried out using the data gained from the third phase of the pumping and reinjection test and the test operation. From the five phases of the pumping and reinjection test only the third phase, with continuous production (05.-08.09.2011), could be used for calibration.

With respect to well WKB Th2 calibration was based on data from the third phase of the pumping and reinjection test and validated by means of data from the pumping test and test operation.

In all calibration runs fluctuations in pumping rates were smoothed by the use of mean values. Only the hydraulic parameters for the Upper Malm unit were varied in the calibration process. In general, the distribution of hydraulic conductivity in the Malm aquifer was assumed to be homogeneous (at a value of 1.5×10^{-6} m/s). However, for specific areas, conductivity values were adjusted. For example, for the fault zone in Malm, hydraulic conductivity of 3.0×10^{-6} m/s was assumed, for the vicinity of the well WKB Th2 a value of 1.0×10^{-6} m/s was used, and for the vicinity of the well WKB Th1, a value of 2.0×10^{-6} m/s. These hydraulic conductivity values represent the initial values of the calibration based on the evaluation of pumping tests (Table 6).

4.4.1 Productivity and injectivity of the wells

Equation (1) describes the drawdown as a function of the pumping rate, taking account of the well loss in WKB Th1.

$$s_w[m] = 2.2583 \cdot Q + 0.002564 \cdot Q^2 \; [l/s] \qquad (3)$$

Owing to the negligible difference between the theoretical and the actual drawdown in WKB Th1 (Figure 7) the calibration of the hydraulic tests was conducted with the measured hydraulic head values. By contrast, in WKB Th2, the injection well loss cannot be neglected and therefore the calibration was made using the theoretical pressure values.

The following equation can be used for the injectivity in well WKB Th2:

$$P[bar] = 0.2832 \cdot Q + 0.0076 \cdot Q^2 \; [l/s] \qquad (4)$$

Figure 8 presents the specific pumping and injection diagram. The theoretical reinjection pressure was calculated and taken as a basis for the calibration in WKB Th2 based on equation (4).

4.4.2 Pumping test in well WKB Th1

The pumping test in WKB Th1 was carried out using an average pumping rate of 52.6 l/s and with moderate fluctuations of the pumping rate. The time series of the pumping rate was schematised by five pumping steps (step 1: 63.7 l/s; step 2: 47.3 l/s; step 3: 56.4 l/s; step 4: 57.3 l/s and step 5: 52.8 l/s). Although the differences between the pumping rates in steps 1 to 2 and 3 to 5 are minor, the drawdown during steps 3 to 5 is disproportionally larger than it is during steps 1 to 2.

Figure 9 indicates that the simulated drawdown in step 1 and 2 fits reasonably well, whereas in steps 3 to 5 the drawdown is smaller, but more plausible, than that measured. (In Figure 9 and Figures 11 to 13 the parameters are: k – hydraulic conductivity of the aquifer, k_{Th1} – hydraulic conductivity in the region of WKB

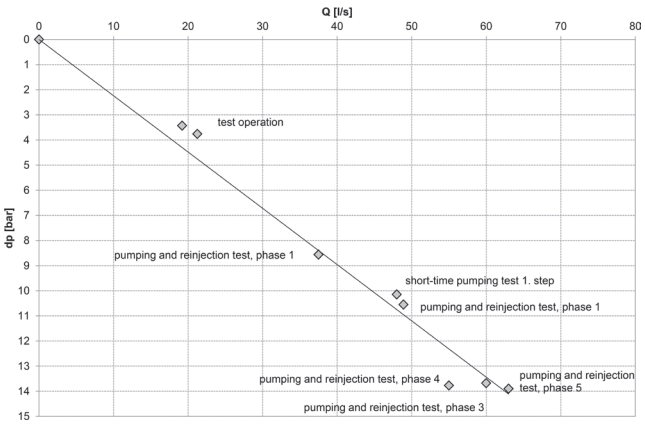

Figure 5: Q – dp diagram of the well WKB Th1

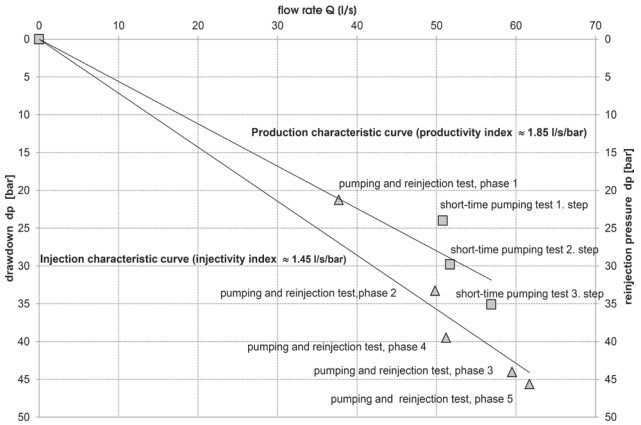

Figure 6: Q – dp diagram of the well WKB Th2.

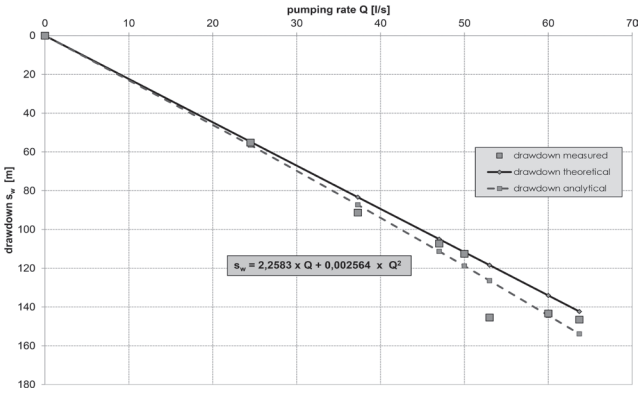

Figure 7: Specific capacity of WKB Th1.

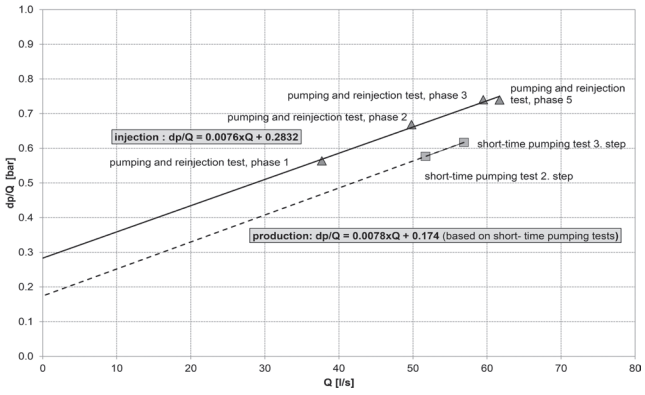

Figure 8: Productivity and injectivity of WKB Th2.

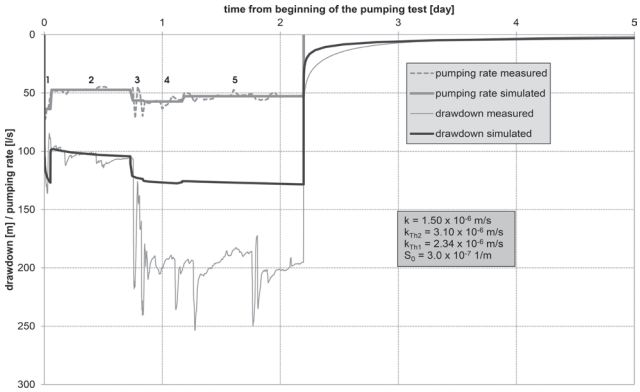

Figure 9: Simulation of the pumping test in WKB Th1.

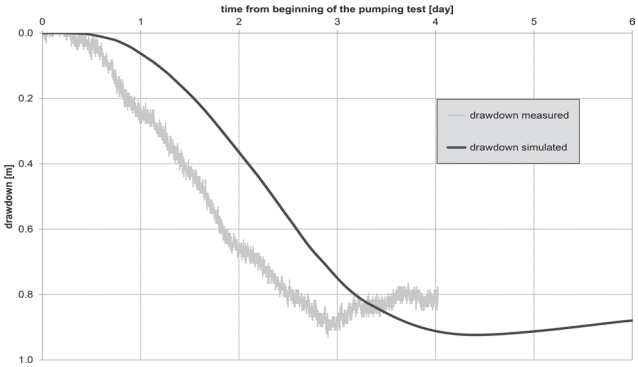

Figure 10: Simulation of the reaction in WKB Th2 to the pumping in WKB Th1.

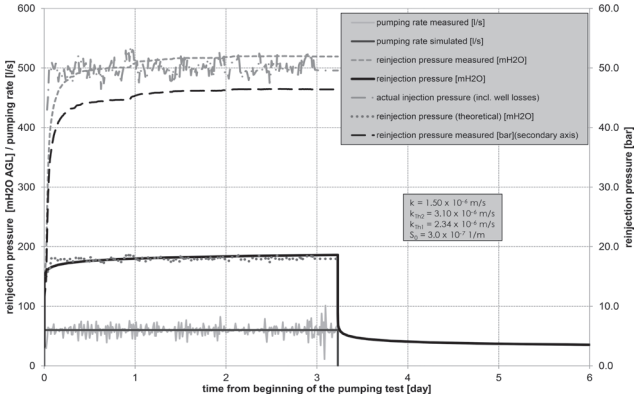

Figure 11: Simulation of phase 3 of the pumping and reinjection test in WKB Th2.

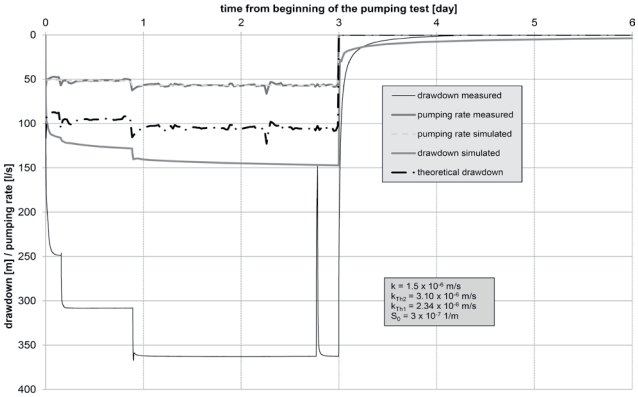

Figure 12: Validation in WKB Th1 by means of phase 3 of the pumping and reinjection test.

Th1, k_{Th2} – hydraulic conductivity in the region of WKB Th2, S_0 – specific storage coefficient of the aquifer). Figure 10 shows the reaction in WKB Th2 to the pumping in WKB Th1. While the overall magnitude of the simulated drawdown time-series corresponds well to that of the measured drawdown, the minimum level of drawdown in the simulation occurs approx. 30 hours later than in the measured drawdown time-series.

4.4.3 Pumping and reinjection test phase 3 in well WKB Th2

The pumping and reinjection test was carried out in five phases subsequent to both short-time pumping tests. Of these five phases, the 3rd phase, which proceeded without any specific problems, was used for the calibration.

The calibration of the simulated reinjection pressure in WKB Th2 is shown in Figure 11. The reinjection pressure measured at the wellhead (in bar), taking into account the temperature of the water, was converted into m water column, thus allowing for comparison with the simulated hydraulic head in WKB Th2.

4.4.4 Calibration results

The aquifer has a general horizontal hydraulic conductivity of kxx,= kyy = 1.5x10^{-6} m/s, the fault running near WKB Th2 exhibits a hydraulic conductivity of 3.0x10^{-6} m/s, in the region of WKB Th2 the conductivity amounts to 3.10x10^{-6} m/s, and in the vicinity of WKB Th1, to 2.34x10^{-6} m/s. The horizontal extent of the hydraulic conductivity zones around the wells WKB Th1 und WKB Th2 was defined with respect to the tested area during the pumping tests. Employing Kusakin´s empirical formula (Bear, 1979), the cone of depression was estimated to be between 1,600 m and 2,400 m around WKB Th1, and to be between 2,900 m and 3,400 m around WKB Th2.

The vertical hydraulic conductivity (kzz) reflects the assumed anisotropy factor and amounts to a fifth of the horizontal hydraulic conductivity.

4.4.5 Validation

The validation process was carried out for different hydraulic tests. The validation by means of phase 3 of the pumping and reinjection test in WKB Th1 revealed an acceptable fit both with respect to the pumping and the recovery period. It is clearly noticeable that a better fit is observed towards the end of these periods (Figure 12).

In WKB Th2 the short-time pumping test was used for validation as this test could be performed without significant fluctuation of the pumping rate (Figure 13). The difference with respect to the theoretical drawdown is obvious. This is because equation (4) was used for the calibration, and the C-factors in the equations for productivity and injectivity differ from each other. Thus, the validation leads to a clearly larger drawdown than could be expected by the productivity.

Validation via test operation yielded differences of a similar

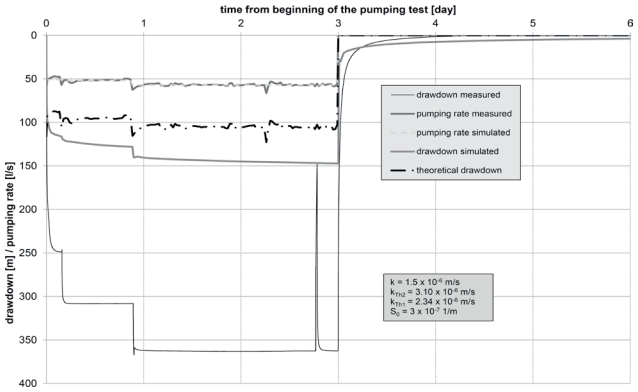

Figure 13: Pumping test validation for WKB Th2.

range. In WKB Th1 the drawdown is overestimated by about 1 bar. This corresponds to the difference between the measuring points for the test operation and the line of best fit in Figure 5. In WKB Th2 the reinjection pressure generally tends to be underestimated, while there is a good level of fit with respect to theoretical values in some sections. Nevertheless, the model can still be accepted as validated.

4.4.6 Thermal parameters and calibration of the conductive temperature field

In the region of the doublet, under average conditions a pressure of some 250 bar and a temperature of 108 °C prevail in the aquifer. Under these physical conditions the rock and the thermal water have the properties presented in Table 8.

Some simple parameters characterising the heat transport in the aquifer can be estimated using the material properties in Table 8. The heat retardation factor R expresses the ratio between the velocity of the groundwater flow and that of the heat front. Thus:

$$R = 1 + \frac{(1-n)\cdot C_R \cdot P_R}{n \cdot c_w \cdot P_w} = 1 + \frac{(1-0.2)\cdot 930 \cdot 2700}{0.02 \cdot 4170 \cdot 964} = 30.6 \quad (5)$$

The heat conduction induced by temperature gradients is considered by a heat diffusion coefficient, whereby the heat conductivity of the aquifer (rock + water) is calculated as a geometric mean of the heat conductivity of rock and that of water.

$$D_{TH} = \frac{\lambda_W^n \cdot \lambda 1_R^{-n}}{(1-n)\cdot p_R \cdot C_R + n \cdot p_w \cdot C_W} = \frac{0.69^{0.02} \cdot 3.3^{1-0.02}}{(1-0.02)\cdot 2700 \cdot 930 + 0.02 \cdot 964 \cdot 4170}$$

$$= 1.26 \cdot 10^{-6} m^2/s \quad (6)$$

The thermo-physical properties of rocks used in the model (Table 9) were set based on the values recommended in the literature (VDI, 2010; ÖWAV, 2009) and took account of the models already prepared and calibrated for the Molasse basin. (Goldbrunner et al., 2008; Wenderoth and Huber, 2011; Dussel et al., 2012).

4.4.7 Dispersivity

With respect to longitudinal dispersivity αL, several authors (Beims, 1983; Bundschuh and Suárez Arriga, 2010) have published diagrams in which results of field experiments on different scales are presented. By means of these diagrams the longitudinal dispersivity for porous aquifers and for an assumed scale of 1 km to 2 km can be estimated to be in the range of 13 to 20 meters. Based on the field experiments described in Reid (1981) the longitudinal dispersivity of limestone is in the range of 6.7 m to 61 m, and that of fractured dolomite is in the range of 3.1 m to 85 m. However, Gelhar et al. (1992) found no significant difference between the longitudinal dispersivities determined for fractured and porous rocks.

The following formula (based on Xu and Eckstein,1995), is used to estimate the longitudinal dispersivity (αL) as a function of field scale (L)

$$\alpha_L = 0.83 \cdot (\log_{10} L)^{2.414} \quad (7)$$

For an estimated field scale of 2 km equation (7) yields a longitudinal dispersivity of 14.8 m. Since the first simulation runs already indicated that a field scale of 2 km was not exceeded, a longitudinal dispersivity of α_L = 15 m and a transversal dispersivity of α_T = 1.5 m were set for the aquifer. In all other layers values of α_L = 5 m and α_T = 0.5 m were assumed.

The calibration of the temperature field was carried out on the basis of temperature measurements in WKB Th1 and WKB Th2. Table 10 shows the uninfluenced temperature values measured in the wells before pumping tests, as well as the calculated temperature values.

When calibrating the temperature field, the model was used to set two thermal boundary conditions: the constant temperature on the top, and the basal heat flux. A mean value of 10 °C was assumed at the top. The starting value of the basal heat flux was estimated on the basis of the geothermal gradient. Assuming an average heat conductivity of the rocks of 2.5 W/m/K this resulted in a value of 0.0975 W/m². Given the assumed operating lifetime of 50 years, the influence of radiogenic heat production in the limestone/dolomite aquifer could be neglected. The material properties shown in Table 9 were used for calibration.

The calibration yielded a basal heat flux of 0.0970 W/m² whereby the basal temperature at a depth of -4,000 m NN varies between 160 °C and 170 °C.

4.5 Simulations

The simulation was conducted using the calibrated and validated model for a simulation period of 50 years. The first

	Density [kg/m³]	Heat conductivity [W/m/K]	Specific heat capacity [J/kg/K]
water	964.0	0.695	4,170
limestone/ dolomite	2,700	3.30	930

Table 8: Thermodynamic properties of rock and water (ÖWAV 2009; VDI 2010; Lemmon et al., 2013).

Geology	Petrography	Model layer	Rock			Water	
			λ_s [W/m/K]	$c_{p,s}$ [x 10^6 J/m³/K]	n [-]	λ_f [W/m/K]	$c_{p,f}$ [x 10^6 J/m³/K]
OFM	gravel, sand	1	2.5	2.25	0.10	0.60	4.20
Neogene	sand, gravel, marl	2	2.5	2.15	0.10	0.61	4.20
Chattian	sand, sandstone, marl	3	2.8	2.15	0.05	0.62	4.20
Lower-Egerian	arg. marl, marlstone, sand, claystone	4	3.0	2.25	0.05	0.63	4.20
Eocene	Lithothamnium limestone, glauconitic marlstone	5	2.8	2.25	0.02	0.64	4.20
Cretaceous	arg marl, carbonate marl	6-9	3.0	2.25	0.02	0.65	4.20
Lower Malm	limestone/dolomite	10-23	3.3	2.10	0.02	0.65-0.68	4.10-4.15
Upper Malm	limestone/dolomite	24-25	2.8	2.20	0.02	0.68	4.10
Crystalline	gneiss/granite	26-28	3.2	2.10	0.01	0.68-0.69	4.00

Table 9: Thermo-physical properties of rock and water (ÖWAV 2009; VDI 2010; Lemmon et al., 2013)

Well	Measuring depth above Top Malm [m]	Measuring depth [m TVD)	Measuring depth [m NN]	Measured temperature [°C]	Geothermal gradient [°C/100 m]	Calculated temperature [°C]
WKB Th1	98	2,363	1,951	101.4	3.87	101.4
WKB Th2	493	1,937	1,525	86.7	3.96	86.8

Table 10: Temperature measurements in WKB Th1 and WKB Th2.

Operation phase	Test operation	Operation
duration [months]	16	584
extraction and reinjection rate [l/s]	20 (0 to 28.5)	65
reinjection temperature [°C]	82.5 (50 to 99)	50

Table 11: Operating data to simulate the doublet operation for 50 years.

Location	Pressure change	Δp [m]
Well		
WKB Th1 (extraction well)	pressure drop	156.2 m (287.3 m NN)
WKB Th2 (reinjection well)	pressure rise	325.6 m (769.1 m NN)
Licence area		
Northern edge	pressure rise	11.8 m
Southern edge	pressure drop	12.3 m
North-western edge	pressure rise	6.4 m
South-western edge	pressure drop	2.8 m
North-eastern edge	pressure rise	3.2 m
South-eastern edge	pressure drop	8.7 m
Model boundary		
Northern boundary	pressure rise	4.2 m
Southern boundary	pressure drop	6.7 m

Table 12: Pressure head changes at different locations and on different scales.

16 months (479 days) represent the test operation (Table 11).

The simulation results allow for the assessment of potential development in both the pumping well WKB Th1 and in the reinjection well WKB Th2, on a local scale (licence area) and on a regional scale (model boundaries).

The simulation results, in terms of relative pressure drop or rise after an operation period of 50 years, are compiled in Table 12. Considering the well losses for an injection rate of 65 l/s in WKB Th2 31.1 bar (i.e. about 328 m) need to be added to the calculated pressure rise.

The horizontal temperature distribution in the middle of the Upper Malm aquifer is presented for the licence area in Figure 14. On the basis of the temperature development a negative temperature impact in WKB Th2 can be excluded, and a thermal breakthrough is not to be expected within 50 years.

To illustrate the spreading of the plume better, the temperature time series of control points along the connecting line between WKB Th1 and WKB Th2 (Top model layer 15) is presented in Figure 15.

To determine the regeneration of the aquifer, and thus the sustainability of exploitation after the doublet 50-year operating lifetime, the simulation was extended to cover a time period of 10,000 years. The temperature time series in WKB Th2

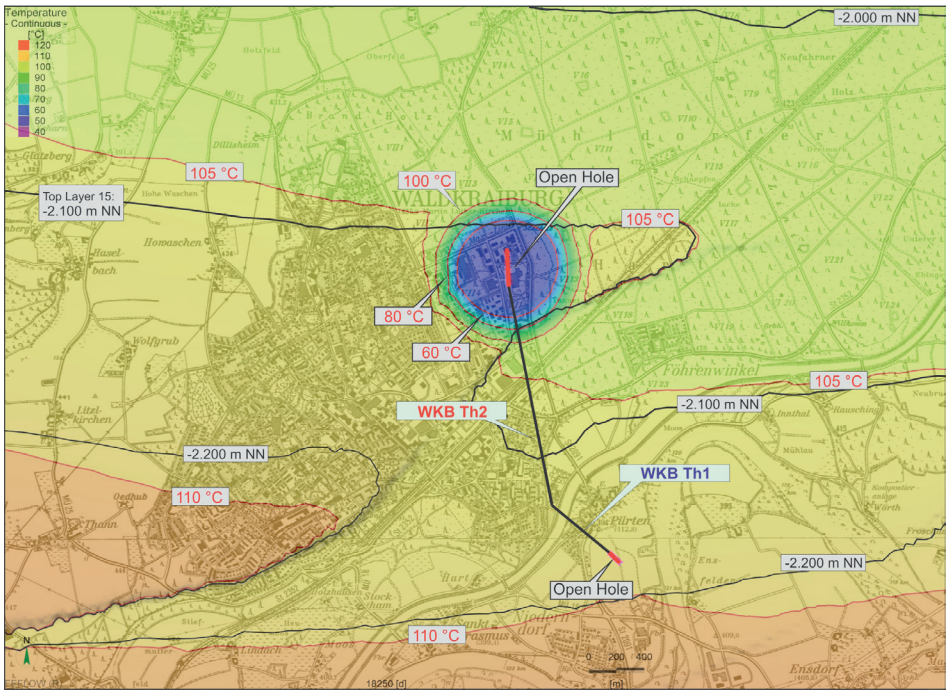

Figure 14: Temperature distribution after 50 years at top of model layer 15.

shows that the temperature rise from 50 °C to 100 °C takes about 2,300 years, and reaches 105 °C (1°C under the initial temperature) after 8,500 years (Figure 16).

4.6 Sensitivity analysis

In order to evaluate the model results and their robustness the main hydraulic and thermal parameters were subjected to sensitivity analysis. The parameters used for the sensitivity analysis were varied, within realistic ranges (VDI, 2010; ÖWAV 2009), in the Upper Malm aquifer (model layer 10 to 23). In the sensitivity analysis the following parameters were included: hydraulic conductivity, specific storage coefficient, dispersivity, porosity, heat conductivity and heat capacity.

In order to evaluate the influence of the different hydraulic and thermal parameters the following characteristic results were chosen: pressure drop/drawdown in the extraction well s [m], reinjection pressure/hydraulic head rise in the injection well h [m], spread of the cold water plume R_{Temp} [m], pressure rise on the northern boundary Δh_{Nb} [m], and pressure drop on the southern boundary Δh_{Sb} [m].

The results are presented as relative values i.e. as differences with respect to the results of the calibrated model (Table 13).

The change in the hydraulic conductivity affects the pressure drop and the pressure rise in the wells considerably, but does not impact the pressure conditions over a wide area. The change in the other parameters shows that no significant effect on the pressure conditions is to be expected in the licence area.

The spread of the cold water plume is influenced significantly by changes in dispersivity and heat capacity. A rise in dispersivity from 15 m to 30 m increases the spread of the cold water plume by 3 %. In the reverse case, when dispersivity falls from 15 m to 7.5 m the spread of the cold water plume decreases by 3 %. Assuming maximum heat capacity for the aquifer rock results in a fall in the spread of the cold water plume by 5 %, while an assumption of minimum heat capacity produces a fall in the cold water plume by 6 %.

5. Results and conclusions

The two deviated drillings, WKB Th1 and WKB Th2 drilled in Waldkraiburg in the fractured limestone-dolomite aquifer (Purbeck-Malm) yielded detailed information about the stratigraphy of the overlaying strata.

The pressure measurements in the wells made an important contribution to updating assessment plans for the Malm aquifer in the area southwest of the Landshut-Neuöttinger High.

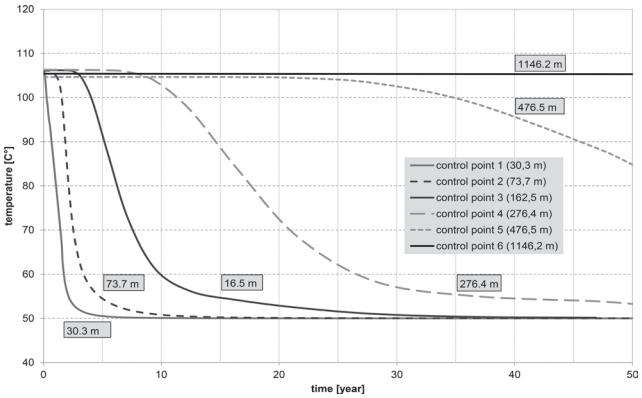

Figure 15: Time series of temperature at top of model layer 15 (mid open-hole).

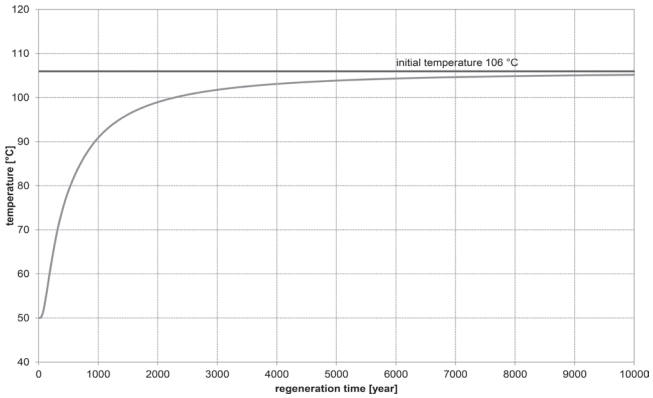

Figure 16: Temperature regeneration in WKB Th2 (at top of model layer 15).

Parameter	Range	h [m]	s [m]	R_{Temp} [m]	Δh_{Nb} [m]	Δh_{Sb} [m]
	Simulation	**325.6**	**156.2**	**537**	**11.8**	**-12.3**
Hydraulic conductivity	$k_{max} = 2 \times k_{kmodel}$	0.501	0.503	1.006	0.517	0.496
	$k_{min} = 0.5 \times k_{model}$	1.997	1.983	0.996	1.847	1.862
Specific storage coefficient	$S_{0,max} = 10 \times S_{0,model}$	1.000	1.000	1.002	1.000	1.000
	$S_{0,min} = 0.1 \times S_{0,model}$	1.000	1.000	1.002	0.992	1.000
Dispersivity	$\alpha_{L,max} = 2 \times \alpha_{L,model}$	0.912	1.000	1.032	1.000	1.000
	$\alpha_{L,main} = 0.5 \times \alpha_{L,model}$	1.000	1.000	0.974	1.000	1.000
Porosity	$n_{max} = 2 \times n_{model}$	1.000	1.000	0.994	1.000	1.000
	$n_{min} = 0.5 \times n_{model}$	1.000	1.000	1.006	1.000	1.000
Heat capacity	$c_{max} = 1.14 \times c_{model}$	0.999	1.000	0.950	1.000	1.000
	$c_{min} = 0.64 \times c_{model}$	1.000	1.000	1.056	1.000	1.000
Heat conductivity	$\lambda_{max} = 1.21 \times \lambda_{model}$	1.000	1.000	1.004	1.000	1.000
	$\lambda_{min} = 0.75 \times \lambda_{model}$	1.000	1.000	1.000	1.000	1.000

Table 13: Relative variation of the characteristic model results.

In the well WKB Th1 the hydraulic potential, assuming model water conditions as defined for the Molasse basin, amounts to 347 m NN. Therefore in the region of Waldkraiburg a reduction by approx. 30 m seems to be essential.

The evaluation of the hydraulic tests allowed the Upper Malm aquifer to be characterised by a transmissivity of 6×10^{-4} m²/s. For a total thickness of the aquifer, hydraulic conductivity of 2×10^{-6} m/s can be assumed, whereby fractured zones may exhibit values five to six times higher. The level of hydraulic conductivity fits the regional zoning in the South German Molasse Basin and corresponds to the values found in the permeable zone (10^{-6} to 10^{-4} m/s). The production temperature of thermal water in WKB Th1 ranges from 106 °C to 108 °C. This temperature range conformed to expectations based upon the geothermal gradient determined for the Ampfing oil field.

Based on a conceptual model, a coupled numerical model was developed in order to simulate the 50-year operation of the geothermal doublet, with an extraction and reinjection rate of 65 l/s and a reinjection temperature of 50 °C.

The simulations and the sensitivity analysis show that the thermal influence of the aquifer (ΔT <1 °C) as a result of the reinjection of cooled water can be predicted to remain within a range of approx. 540 m of reinjection. Thus, no thermal influence is to be expected after an operating period of fifty years and the thermal influence definitely remains restricted to the licence area.

The pressure changes on the boundary of the licence area after a 50-year-operation are not expected to exceed 1.2 bar (northern boundary: +11.8 m; southern boundary: -12.3 m).

In the extraction well, a pressure drop of 156.2 m, and in the reinjection well, a calculated pressure rise of 325.6 m, are to be expected. Considering the injectivity of the reinjection well the predicted reinjection pressure amounts to 64 bar.

Acknowledgements

The authors thank Dr. Thomas Fritzer (Bayerisches Landesamt für Umwelt, Augsburg) for his valuable suggestions regarding model calibration and validation.

The authors would also like to thank the reviewers Prof. Dr. Ingrid Stober and Dr. Peter Bayer for their constructive comments. These proved to be a great help in improving the manuscript.

References

Agemar, T., Weber, J. and Schulz, R., 2014. Deep Geothermal Energy Production in Germany. Energies, 7, 4397-4416. http://dx.doi.org/10.3390/en7074397

Bear, J., 1979. Hydraulics of groundwater. McGraw-Hill International, New York, 567 pp.

Beims, U., 1983. Planung, Durchführung und Auswertung von Gütepumpversuchen. Geohydrodynamische Erkundung. Zeitschrift für Angewandte Geologie 29/10, 484-492.

Birner, J., Fritzer, T., Jodocy, M., Savvatis, A., Schneider, M. and Stober, I., 2012. Hydraulische Eigenschaften des Malmaquifers im Süddeutschen Molassebecken und ihre Bedeutung für die geothermische Erschließung. Zeitschrift für Geologische Wissenschaften., 40:2-3 133-156, Berlin.

Bundschuh, J. and Suárez Arriga, M. C., 2010. Introduction to the Numerical Modeling of Groundwater and Geothermal Systems. Fundamentals of Mass, Energy and Solute Transport in Poroelastic Rocks, CRC Press, Taylor & Francis Group, A. Balkema, Boca Raton, London, New York, Leiden, 479 pp.

De Marsily, G., 1986. Quantitative Hydrogeology. Groundwater Hydrology for Engineers. Academic Press, London, 440 pp.

DHI-WASY 2010. FEFLOW® 6. Finite Element Subsurface Flow & Transport Simulation System. User Manual. DHI-WASY GmbH., Berlin. 94 pp.

Diersch, H.-J., 2014. FEFLOW. Finite Element Modeling of Flow, Mass and Heat Transport in Porous and Fractured Media, Springer, Berlin, 996 pp.

Dussel, M., Lüschen, E., Schulz, R., Thomas, R., Wenderoth, F., Fritzer, T., Birner, J., Schneider, M., Wolfgramm, M., Bartels, J.,

Huber, B., Megies, T. and Wassermann, J., 2012. Geothermische Charakterisierung von karstig-klüftigen Aquiferen im Großraum München. Unpublished report, Leibnitz-Institut für Angewandte Geophysik, Hannover, 98 pp.

Frisch, H. and Huber, B., 2000. Ein Hydrogeologisches Modell und der Versuch einer Bilanzierung des Thermalwasservorkommens für den Malmkarst im Süddeutschen und im angrenzenden Oberösterreichischen Molassebecken. Hydrogeologie und Umwelt, 20, 25-43.

Gelhar, L.W., Welty, C. and Rehfeldt, K.R., 1992. A critical review of data on filed-scale dispersion in aquifers. Water Resources Research, 28/7, 1955-1974. http://dx.doi.org/10.1029/92WR00607

GBA, Geologische Bundesanstalt (ed.) 2103. Geologie von Österreich. Posterkarte. Geol. B.-A. Wien.

Goldbrunner, J., 2012. Geothermie-Erschließungen im Oberösterreichischen Molassebecken. Beiträge zur Hydrogeologie, 59, 87-102.

Goldbrunner, J., Shirbaz, A., Huber, B. and Wenderoth, F., 2008. Dublette Simbach-Braunau Wärmebergbau-Gutachten. Hydrogeologisches Systemmodell und numerische Modellierung. Unpublished report, Geoteam Ges.m.b.H., Gleisdorf, 67 pp.

Jones, T.A., Hamilton, D.E., and Johnson, C.R., 1986. Contouring Geologic Surfaces With The Computer. – Van Nostrand, New York, 314 pp.

Kraus, L., 1968. Lagerungsverhältnisse (Tektonik) und Reflexionsseismik. – In: Erläuterungen zur Geologischen Karte von Bayern 1:25.000, Bl. Nr. 7837 Markt Schwaben, 76-81, München.

Lemcke, K., 1988. Das Bayerische Alpenvorland vor der Eiszeit. Erdgeschichte – Bau – Bodenschätze (Geologie von Bayern. Bd. 1), Schweizerbart´sche Verlagsbuchhandlung, Stuttgart, 175 pp.

Lemmon, E.W., Mclinden, M.O. and Friend, D.G., 2013. „Thermophysical Properties of Fluid Systems" in NIST Chemistry WebBook, NIST Standard Reference Database Number 69. – Eds. P.J. Linstrom and W.G. Mallard, National Institute of Standards and Technology, Gaithersburg MD, 20899, http://webbook.nist.gov, (retrieved February 26, 2013).

Mietens, R., 1966. Geologie, Hydrodynamik, Hydrochemie und Lagerstättenbildung im Wasserburger Trog der ostbayrischen Tafelmolasse. Doctoral Thesis, Technische Universität Clausthal, Germany 106 pp.

ÖWAV, Österreichischer Wasser- und Abfallwirtschaftsverband 2009. Thermische Nutzung des Grundwassers und des Untergrunds – Heizen und Kühlen. ÖWAV-Regelblatt 2007, ÖWAV Wien, 68 pp.

Reid, G.C., 1981. Literature evaluation of induced groundwater tracers, field tracer techniques, and hydrodynamic values in porous media. Master Thesis, Texas Technical University, 102 pp.

Stober, I., 1995. Die Wasserführung des kristallinen Grundgebirges. Ferdinand Enke Verlag, Stuttgart, 191 pp.

Stober, I., Wolfgramm, M. and Birner, J., 2014. Geothermale Tiefenwässer in Deutschland. – Hintergrundpapier des GtV-Bundesverbandes Geothermie, Berlin, 21 pp.

Unger, H.J., 1978. Geologische Karte von Bayern 1:50.000. Erläuterungen. Blatt Nr. L 7740 Mühldorf am Inn. Bayer. Geol. LA., München, 184 pp.

VDI, Verein Deutscher Ingenieure 2010. Thermische Nutzung des Untergrundes. Grundlagen, Genehmigungen, Umweltaspekte. VDI 4640, Blatt 1, Düsseldorf, 31 pp.

Wagner, B., Kus, G., Kainzmaier B., Spörlein, T., Wilferth, T., VEIT, W., Fritsch, P., Wrobel, M., Lindenthal, W., Neumann, J., and Sprenger, W., 2009. Erläuterungen zur Hydrogeologischen Karte von Bayern 1:500.000. Bayerisches Landesamt für Umwelt, Augsburg, 88 pp.

Wenderoth, F. and Huber, B., 2011. Geothermieprojekt „Neukirchstockach". Gutachten über den Wärmebergbau im Untergrund. Unpublished report, AQUASOIL GmbH. und HydroConsult GmbH., Berlin-Augsburg, 55 pp.

Xu, M. and Eckstein, Y., 1995. Use of weighted least-squares method in evaluation of the relationship between dispersivity and field scale. Ground Water, 33:6, 905-908. http://dx.doi.org/10.1111/j.1745-6584.1995.tb00035.x

Received: 18 May 2015
Accepted: 12 November 2015

Johann E. GOLDBRUNNER[1)] & Vilmos VASVÁRI[2)]

[1)] Geoteam Ges.m.b.H., Bahnhofgürtel 77/IV, 8020 Graz, Austria;

[2)] Ingenieurbüro für Kulturtechnik und Wasserwirtschaft, Kleegasse 4, 8020 Graz, Austria, office@ib-vasvari.at;

[*)] Corresponding author, goldbrunner@geoteam.at